Published in final edited form as:

Toxicol Sci. 2022 April 26; 187(1): 139–149. doi:10.1093/toxsci/kfac014.

Characterization of the mechanistic linkages between iodothyronine deiodinase inhibition and impaired thyroid-mediated growth and development in *Xenopus laevis* using iopanoic acid

Jonathan T. Haselman[1,*], **Jennifer H. Olker**[1], **Patricia A. Kosian**[1,2], **Joseph J. Korte**[1,2], **Jeffrey S. Denny**[1,2], **Joseph E. Tietge**[1,2], **Michael W. Hornung**[1], **Sigmund J. Degitz**[1]

[1]U.S. Environmental Protection Agency, Office of Research and Development, Center for Computational Toxicology and Exposure, Great Lakes Toxicology and Ecology Division, Duluth, Minnesota 55804

[2]Retired

Abstract

Iodothyronine deiodinases (DIO) are key enzymes that influence tissue-specific thyroid hormone levels during thyroid-mediated amphibian metamorphosis. Within the larger context of evaluating chemicals for thyroid system disrupting potential, chemical activity toward DIOs is being evaluated using high-throughput in vitro screening assays as part of U.S. EPA's ToxCast program. However, existing data gaps preclude any inferences between in vitro chemical inhibition of DIOs and in vivo outcomes relevant to ecological risk assessment. This study aimed to generate targeted data in a laboratory model species (*Xenopus laevis*) using a model DIO inhibitor, iopanoic acid (IOP), to characterize linkages between in vitro potency, in vivo biochemical responses, and adverse organismal outcomes. In vitro potency of IOP toward DIOs was evaluated using previously developed in vitro screening assays, which showed concentration-dependent inhibition of human DIO1 (IC_{50}: 97 μM) and DIO2 (IC_{50}: 231 μM) but did not inhibit human or *X. laevis* DIO3 under the assay conditions. In vivo exposure of larval *X. laevis* to 0, 2.6, 5.3 and 10.5 μM IOP caused thyroid-related biochemical profiles in the thyroid gland and plasma consistent with hyperthyroxinemia but resulted in delayed metamorphosis and significantly reduced growth in the highest two exposure concentrations. Independent evaluations of *dio* gene expression ontogeny, together with existing literature, supported interpretation of IOP-mediated effects resulting in a proposed adverse outcome pathway for DIO2 inhibition leading to altered amphibian metamorphosis. This study highlights the types of mechanistic data needed to move toward predicting in vivo outcomes of regulatory concern from in vitro bioactivity data.

[*]**Corresponding author:** Jonathan Haselman, 218-529-5244, haselman.jon@epa.gov; U.S. EPA, Great Lakes Toxicology and Ecology Division, Duluth, Minnesota 55804.

Financial Interest Declaration: The authors declare they have no actual or potential competing financial interests.

Keywords

Thyroid; *Xenopus laevis* ; Iodothyronine deiodinase; Adverse Outcome Pathway; Endocrine disruption

INTRODUCTION

Chemical hazard assessment for thyroid system disrupting chemicals is transitioning from reliance on traditional animal testing to increased utilization of alternative methods such as in vitro screening of chemical activity toward specific molecular targets (Hornung et al., 2018; Olker et al., 2019; Wang et al., 2018, 2019, 2021; Paul Friedman et al., 2016, 2019). Efforts are underway to screen large chemical libraries for activity toward thyroid-related molecular targets and interpret the potential impacts in the context of Adverse Outcome Pathways (AOPs) leading from the molecular initiating event (MIE), or in vitro activity, to an adverse outcome (AO) relevant to regulatory risk assessment (Noyes et al., 2019). Ecological risk assessment is primarily based on apical AOs such as growth, development, and reproduction, which are evaluated using regulatory in vivo test guidelines. While mechanistic-based high-throughput in vitro screening can characterize chemical interactions with proteins and cell systems, it lacks defined relationships to AOs of regulatory concern. Delineation of AOPs provides a scientific basis for interpreting and prioritizing both in vitro targets themselves and chemical activity toward those targets. A significant challenge faced by the transition to non-animal chemical hazard assessment is the paucity of intermediate biochemical response data supporting the mechanistic linkages between in vitro activity and apical organismal effects.

The objective of this study was to characterize intermediate biochemical responses leading from deiodinase enzyme inhibition to apical, organismal-level impacts in the model amphibian *Xenopus laevis*, a species utilized internationally to evaluate chemical effects on thyroid-mediated metamorphosis (OECD, 2009, 2015; U.S. EPA, 2009, 2015). Deiodinase enzyme systems are highly conserved across vertebrate species and integral to regulating highly localized thyroid hormone (TH) levels in cells and tissues. During amphibian metamorphosis, types 1, 2 and 3 deiodinase (DIO1, DIO2, DIO3) enzymes are differentially expressed in peripheral tissues and serve to metabolically activate and inactivate THs depending on the specific functional requirements of the cell and/or tissue at the time (Brown, 2005). The function of DIO2 is to metabolically activate prohormone, thyroxine (T4), by removing an outer ring iodine to yield triiodothyronine (T3), the active TH receptor ligand. The function of DIO3 is to inactivate T4 and/or T3 by removing an inner ring iodine to produce inactive hormone species, reverse T3 (rT3) and/or T2, respectively. DIO1 generally has both inner and outer ring deiodination capabilities but appears to lack relevance during amphibian metamorphosis (Kuiper et al., 2006).

Iopanoic acid (IOP) is an oral cholecystographic agent that has been well-characterized as a DIO1 and DIO2 inhibitor (Braga and Cooper, 2001) and acts as a substrate of DIO1 (Renko et al., 2012). IOP was used as a model DIO inhibitor as part of the global harmonization and validation of the Amphibian Metamorphosis Assay (AMA) through the Organization of

Economic Cooperation and Development (OECD, 2007). IOP has also been utilized as a xenobiotic inhibitor of DIO enzymes in vivo to characterize the roles of T3 and T4 in *Rana catesbeiana* thyroid-mediated metamorphosis (Galton, 1989; Becker et al., 1997). Although these studies emphasize the importance of DIOs in amphibian metamorphosis, the data have not been assembled in a manner directly supporting the mechanistic relationships between perturbed biochemistry and metamorphic dysfunction. Assembly of the data in a manner to support those mechanistic relationships using a model chemical and a model amphibian species aids interpretation and prioritization of other chemicals showing in vitro bioactivity toward DIOs.

In this study, constitutive gene expression ontogeny and in vitro DIO inhibition by IOP are considered in the context of in vivo TH levels and apical outcomes caused by exposure to IOP. Constitutive gene expression ontogeny of the *dio* isoforms was characterized throughout metamorphosis in pituitary, thyroid, liver, and hind limb to understand the spatiotemporal patterns of putative DIO presence in these key tissues. Relative inhibition of the DIO isoforms by IOP was also assessed using a modified in vitro screening assay involving liquid chromatography-tandem mass spectrometry (LC-MS/MS). This modified approach was necessary to circumvent iodine interference from IOP when using the original screening assay methodology. Lastly, a targeted in vivo exposure was conducted with pro-metamorphic *X. laevis* using an extended AMA study design. Larvae were exposed to IOP throughout metamorphosis and subsamples were taken at multiple timepoints to evaluate key biochemical profiles to better understand the predominant systemic impact of DIO inhibition. Quantitative and qualitative assessments of apical outcomes such as growth and developmental rates were also performed to interpret linkages between early biochemical impacts and apical adverse outcomes resulting in a proposed AOP for DIO2.

MATERIALS AND METHODS

In vitro deiodinase enzyme inhibition assays

Our lab had already developed and implemented in vitro enzyme inhibition assays for recombinant human types 1, 2 and 3 iodothyronine deiodinases (hDIO1, hDIO2, hDIO3), so these assays were utilized for this study with the assumption that relative inhibition by IOP would be similar across species (Hornung et al., 2018; Olker et al., 2019). A recombinant *X. laevis* type 3 DIO (xDIO3) assay had also been developed and implemented in our lab to evaluate potential species differences in relative potency of a subset of chemicals toward DIO3 (Mayasich et al., 2021). Efforts to develop in vitro assays for *X. laevis* types 1 and 2 deiodinases were not successful. The in vitro assays utilized in this study were conducted under similar conditions as those described previously for screening U.S. EPA's ToxCast chemical libraries (Hornung et al., 2018; Mayasich et al., 2021; Olker et al., 2019). However, since IOP is both iodinated and acts as a DIO substrate (hDIO1; Renko et al., 2012), the iodine liberated from IOP interferes with these assay readouts which rely upon the concentrations of free iodine released from iodothyronine substrates. As such, IOP was not evaluated as part of the initial ToxCast screening efforts. To assess inhibition of DIOs by IOP, similar enzyme inhibition assay conditions were used except the expected product formation was quantified as the assay readout using an LC-MS/MS method. Reactions

were stopped at 180 minutes with a volume of stop solution (4% formic acid and 20% acetonitrile) equal to the volume of the reaction. The resulting samples were diluted 500- to 1500-fold so that determinations of product formation (i.e., T2 and T3) were within the range detectable by the LC-MS/MS method (~ 0.03 to 20 nM). The sources of human and *X. laevis* recombinant enzyme activity (cell homogenates) are the same as those used by Hornung et al. (2018), Mayasich et al. (2021) and Olker et al. (2019).

The final assay conditions for each of the four assays are summarized in Supplemental Table S1. IOP and model inhibitors (DIO1: propylthiouracil [PTU]; DIO2, DIO3: xanthohumol [XTH]) were dissolved in DMSO and tested at 400, 100, 20, 8, 4, 0.8, and 0.16 μM in all four assays with the final DMSO concentration being 1% in all wells. A solvent control of DMSO-only was also tested and considered maximal enzyme activity. Initially, enzyme and buffer were combined with each concentration of IOP, model inhibitor or DMSO-only. The reaction was then initiated by adding a master mix with substrate and the other reagents. The plate was sealed, mixed and incubated at 37°C for 180 minutes. A 40 μl aliquot was transferred to a new 96-well plate and 40 μl of stop solution was immediately added, the plates were mixed and placed on ice. All samples were transferred to −80°C until solid phase extraction and analysis by LC-MS/MS for 3,3'-T2 (DIO1 and DIO3 product), or T3 (DIO2 product).

To determine product concentrations, samples (80 μl) were removed from the freezer, thawed on ice and 5 μl were added to either 2.5, 5 or 7.5 ml of 2% formic acid, 5.5% acetonitrile (ACN) (aq) for 1:500, 1:1000 or 1:1500 dilutions, respectively, depending on the expected product concentrations. Dilutions were vortex mixed and 500 μl transferred to respective wells in 96-well plates. The samples were then spiked with a stable isotope internal standard solution (^{13}C6-T2, ^{13}C6-T3, ^{13}C6-rT3, ^{13}C6-T4). The acidified samples were processed through cation exchange (CX) solid phase extraction (SPE) using methods previously described (Hassan et al., 2017). The dried SPE extracts were reconstituted with 100 μl of 25% ACN:75% H_20 (v/v), transferred to micro-sampling vials (Agilent Technologies) and analyzed for iodothyronines using LC-MS/MS as described in Hassan et al. (2017).

In vivo exposure study design

Nieuwkoop and Faber (NF; 1994) stage 54 (pro-metamorphic) *X. laevis* larvae underwent aqueous exposure in flow-through conditions to iopanoic acid (IOP) at nominal concentrations of 1.5, 3.0 and 6.0 mg/L, which correspond to 2.63, 5.25 and 10.5 μM, respectively. Concentrations used in this study were based on the concentrations used in the OECD Phase II interlaboratory validation study where measurable effects on thyroid-mediated metamorphosis were generally consistent across five independent laboratories (OECD, 2007). The balanced design included a control treatment of Lake Superior water (LSW) only. All treatments and control contained three replicate exposure tanks, each starting with 40 larvae. To capture temporal thyroid-related biochemical perturbations during pro-metamorphosis, 8 randomly selected larvae per tank were sampled on both days 7 and 11 for blood plasma and thyroid glands. Each of the 8 larvae had their two thyroid glands divided and evenly distributed to a pool per tank for each sodium-iodide symporter

(*nis*) gene expression and iodo-tyrosine/thyronine analyses for even representation of all 8 larvae in each pool. Transcript abundance of *nis* in thyroid glands was evaluated as a surrogate indicator of gland stimulation by thyroid stimulating hormone (TSH). Iodo-tyrosine/thyronine quantification in the thyroid glands was a direct measure of iodine organification by thyroperoxidase and TH-related synthesis products that can also be indicative of gland stimulation. The remaining larvae continued exposure throughout the remainder of the test. Observations and any mortalities were recorded daily in addition to the date on which each larva completed metamorphosis, which is defined by NF guidelines as the lack of visible tail remnants when the individual is viewed ventral side up. The study was terminated one week after the last control larva completed metamorphosis (day 42). All individuals were weighed, a subset was imaged, and developmental abnormalities were assessed and documented; no blood, gland or tissue samples were taken from metamorphosed froglets.

Animals, study initiation and environmental conditions

X. laevis larvae were acquired from a single spawn resulting from the in-house breeding colony. All animal care and use procedures were reviewed and approved by the IACUC. Study initiation procedures with NF stage 54 larvae, feeding and environmental conditions throughout the test followed methods previously described by Haselman et al. (2020). Water quality parameters did not differ significantly within or between treatments nor over the duration of the study, so all data are summarized together in Supplemental Table S2.

Sample collection and handling

At 7 and 11 days of exposure, 8 larvae were randomly removed from each exposure and control tank and immediately processed sequentially. Sampling, which including euthanasia, weights, developmental staging and blood collection, were performed according to procedures previously described by Haselman et al. (2020). Immediately following blood collection, two thyroid glands were removed from each larva and each gland was randomly distributed to one of two pools for each replicate test tank. One gland was transferred to one 1.5 mL microcentrifuge tube for *nis* gene expression analyses (n = 8 glands), which was kept on dry ice throughout the sampling period, and the other gland was transferred to another 1.5 mL microcentrifuge tube for iodo-tyrosine/thyronine quantification (n = 8 glands), which was kept on wet ice throughout the sampling period. All pooled plasma and thyroid gland samples were transferred to −80°C storage until further processing.

Chemical stock preparation and exposure verification

Iopanoic acid (CAS# 96-83-3; purity >98%; TCI America, Portland, OR, USA) stocks were prepared from neat material weekly. 12 g IOP was added to 500 mL 0.1 M sodium hydroxide and stirred until completely dissolved. This solution was quantitatively transferred to approximately 17 L of LSW and titrated with hydrochloric acid to pH 8.0. The total volume was then brought up to 19 L. The stock was diluted and delivered to the test tanks with an automated ratio-pump dilution system. To verify exposure concentrations, test tank samples (0.5 mL) were collected weekly, transferred into amber colored HPLC vials, and diluted with 0.5 mL of HPLC grade ACN. The samples were then immediately vortexed and analyzed using an Agilent 1100 series high performance liquid chromatograph (HPLC)

using diode array detection (λ = 231 nm). A 50 μL aliquot of sample was injected into a LiChrosorb RP-18 column (5 μm particle size, 100 mm × 4.6 mm) maintained at 23°C. IOP was eluted using isocratic conditions of 25% Burdick & Jackson water (B&J) HPLC grade water, 75% B&J HPLC grade ACN with 10 mM acetic acid, at a flowrate of 1.0 mL/min. IOP chemical concentrations were quantified using external standards (0.2 to 8 mg/L in 50% B&J water, 50% B&J ACN with 10 mM acetic acid) with linear regression. Quality assurance samples were prepared for each sample set, consisting of LSW blanks, duplicate samples and matrix spiked samples at corresponding concentrations for each treatment. IOP was not detected in the LSW blanks (n = 6). Mean ± SD (n = 6) concentration agreement with duplicate samples were 100.1 ± 0.3%, 100.0 ± 0.1%, and 100.3 ± 0.5% for 1.5, 3.0, and 6.0 mg/L treatments, respectively. Mean ± SD (n = 6) recoveries of spiked samples were 98.9 ± 3.4%, 101.1 ± 2.2%, and 99.5 ± 1.3% for 1.5, 3.0, and 6.0 mg/L spiked concentrations, respectively. Mean ± SD (n = 18) IOP concentrations for the LSW control, 1.5, 3.0 and 6.0 mg/L treatments were 0.00 ± 0.00, 1.63 ± 0.05, 3.27 ± 0.09, and 6.49 ± 0.17 mg/L, respectively, over the course of the exposure. The method limit of detection was 0.1 mg/L. The coefficient of variation for each treatment was 2.88%, 2.64%, and 2.60% for 1.5, 3.0, and 6.0 mg/L treatment levels, respectively.

Iodotyrosines/iodothyronines in plasma and thyroid glands

Iodinated amino acid species (monoiodotyrosine [MIT], diiodotyrosine [DIT], 3,3',5 triiodothyronine [T3], 3,3',5' triiodothyronine [rT3], thyroxine [T4]) were quantified in plasma and thyroid glands using sample preparation methods and LC-MS/MS as previously described (Hassan et al., 2017; Hornung et al., 2015; Olker et al., 2018). Briefly, plasma pools (n = 3 per treatment and control) were subjected to acid hydrolysis to free protein-bound TH prior to further processing through SPE. Thyroid gland pools (n = 3 per treatment and control) were sonicated in Tris/EDTA buffer to homogenize the tissue, digested with pronase to liberate iodotyrosines and iodothyronines from thyroglobulin and then further processed through SPE. SPE extracts were reconstituted in appropriate matrices and analyzed using an Agilent 6490 Triple Quadrupole LC-MS/MS and Agilent Mass Hunter software. The lower limits of quantitation (LLOQ) for plasma MIT, DIT, T3, rT3 and T4 were 0.8, 0.1, 0.2, 0.08 and 0.06 nM, respectively. The LLOQs for gland extract MIT, DIT, T3, rT3 and T4 were 0.2, 0.03, 0.008, 0.02, 0.02 pmole/gland, respectively.

RNA extraction and gene expression analyses.

Thyroid gland nis expression.—Three biological replicates per treatment and control, each consisting of 8 pooled thyroid glands by tank were lysed, homogenized and processed to extract total RNA using buffers and procedures according to RNeasy® Plus Micro kit instructions (Qiagen, Germantown, MD, USA). Evaluation of RNA quality, quantity and absolute quantitation of *nis* mRNA and normalizing gene *rpl32* mRNA by QPCR were performed according to methods previously described (Haselman et al., 2020; Olker et al., 2018; Sternberg et al., 2011; Tietge et al., 2013). Briefly, duplexed real-time QPCR reactions were set up with sequence-specific primers and probes labeled with a 5' 6-FAM fluorophore for *nis* and Cy5 for *rpl32* (Integrated DNA Technologies, Coralville, IA) using a one-step TaqMan EZ RT-PCR assay kit (Applied Biosystems, Foster City, California) on a 7500 Real-time PCR Detection System (Applied Biosystems). Numbers of mRNA copies

for each transcript were determined using known quantities of standard templates generated according to methods previously described (Sternberg et al., 2011; Tietge et al., 2013).

Developmental gene expression ontogeny.—*X. laevis* pituitary, thyroid glands, liver and limbs were collected from an independent untreated spawn at various stages of pro-metamorphic development and gene expression of *dio1*, *dio2.L* and *dio3.L* were measured. RNA extractions, quality and quantity assessments and gene expression measurements by QPCR were performed according to procedures described above for *nis* gene expression except that tissue samples were collected and processed on an individual basis and the *dio* expression levels were normalized to total RNA instead of a reference gene (n = 5, 4, 5, 5 per NF stage for pituitary, thyroid, liver and limb, respectively). In some cases, the amount of total RNA was very low and close to the limit of detection of the spectrophotometer, so normalized expression values may be disproportionally underestimated for transcripts of low abundance. However, despite potential inaccuracies in the absolute abundance of mRNAs, the data nonetheless reflect relative abundances of transcripts throughout a critical period of thyroid-mediated development. Primers and probe sequences used are provided in Supplemental Table S3.

Data analyses and statistics

In vitro enzyme inhibition.—Relative concentrations of product were baseline adjusted based on the product concentrations present in the highest model inhibitor concentration (i.e., mean product concentrations in the highest model inhibitor concentration were subtracted from all replicate wells). Then, data were expressed and analyzed as a percent of maximum activity by normalizing the baseline-adjusted product concentrations to the mean product concentration in the DMSO-only wells, which were considered maximum (100%) enzyme activity. All biological replicates (n = 3) were normalized individually to the corresponding DMSO-only mean per enzyme assay and the median with min/max activity for the three replicates are reported following previously described methods (Hornung et al., 2018; Mayasich et al., 2021; Olker et al., 2019). Data were fitted to a dose-response model and IC_{50} estimates were acquired using R (R core team, 2020) and the drc v3.0-1 package (Ritz et al., 2015).

In vivo exposure.—Input data for statistical analyses consisted of a single value per replicate tank for biochemical and growth endpoints (n = 3). For biochemical measurements, blood and tissues were pooled by tank prior to making a single measurement from the pool, while larval mass was measured for every sampled individual in each tank and averaged. Developmental rates (days to NF 66) were collected for every remaining larva following the 11-d sampling and all individuals were treated as inputs for statistical analysis (described below); however, these data were summarized by calculating the mean of replicate tank medians. All analyses were performed using R (R core team, 2020); specific packages are referenced accordingly. Using the StatCharrms v0.90.96 package (Swintek et al., 2017), data from each endpoint and timepoint were rank transformed, fitted to an ANOVA model and monotonicity was evaluated by comparing linear and quadratic contrasts. Monotonic data were analyzed for significant differences between treatments and control using the step-down Jonckheere-Terpstra trend test. Only one dataset did not meet assumptions of

monotonicity (*nis* gene expression at 11 d); this dataset was evaluated for normality and homogeneity of variance using the Shapiro-Wilk (stats; R core team, 2020) and Levene's test (car v3.0-8; Fox and Weisberg, 2019), respectively. Having met parametric assumptions, these data were evaluated for differences between treatments and control using a one-way ANOVA model with Dunnett's post-hoc test. To determine differences in developmental rates, days to completion of metamorphosis were treated as time-to-event data and analyzed using a Cox mixed-effects proportional hazard model (coxme v2.2-16; Therneau, 2020) with individuals not reaching NF stage 66 censored within the analysis. An alpha level of 0.05 was used as the upper threshold, below which treatments were considered significantly different than control.

RESULTS

In vitro enzyme inhibition

Inhibition of iodothyronine deiodinase enzymes was evaluated using recombinant human isoforms (hDIO1, hDIO2 and hDIO3). Recent work utilizing recombinant *X. laevis* DIO3 (xDIO3) for in vitro enzyme inhibition assays (Mayasich et al., 2021) enabled an orthologous comparison of potential IOP inhibition of inner ring deiodination (i.e., TH inactivation). IOP inhibited hDIO1 and hDIO2 with IC_{50} concentrations of 97 μM and 231 μM, respectively, for these assay conditions (Figure 1A & 1B). IOP did not inhibit hDIO3 nor xDIO3 – these data were consistent across orthologous assays and both exhibited slight elevations of product formation in the highest IOP concentrations (Figure 1C & 1D). The hDIO1 model inhibitor, PTU, produced an IC_{50} of 0.3 μM using this method (Figure 1A). The hDIO2 and hDIO3 model inhibitor, XTH, produced IC_{50}s of 0.27 and 0.14 μM, respectively (Figure 1B & 1C). The XTH IC_{50} for xDIO3 was 0.13 μM (Figure 1D). If inhibition of the human DIO orthologs by IOP in vitro is reasonably predictive of IOP's potency toward *X. laevis* DIOs, then IOP indeed shows potential to inhibit DIO1 and/or DIO2 in vivo. These data provide the toxicological basis for these enzymes being identified as putative MIEs in the AOP framework.

Growth and development

Body mass was significantly decreased compared to control on day 11 and at NF stage 66 (i.e., completion of metamorphosis) in the 3.0 and 6.0 mg/L IOP treatments with the highest treatment being less than half the size of control on average for those that achieved NF stage 66. There were concurrent delays of metamorphic development in the 3.0 and 6.0 mg/L treatments, as it took 28 and 32 days to reach NF stage 66, respectively, compared to 27 days in control (Table 1). Minimal mortality was observed throughout the duration of the study and was not concentration-dependent (Table 1). Approximately half of the larvae in the 6.0 mg/L treatment did not achieve NF stage 66 within the duration of the study (42 days), whereas all remaining larvae in the other treatments and control achieved NF stage 66 (Table 1). Notable qualitative observations included precocious initiation of tail resorption, delayed/arrested gill resorption, and abnormal head remodeling (i.e., overall asynchronous development [images not shown]) in the 3.0 and 6.0 mg/L treatments around days 20–25 (metamorphic climax; NF stage 62) with a subsequent delay in completion of full tail resorption beyond metamorphic climax (images not shown). Most larvae that

achieved NF stage 66 in the 6.0 mg/L treatment retained a minute amount of tail tissue that was only visible dorsally. Asynchronous development presented as deviations from expected morphological changes based on typical sequence of metamorphic progression of somatic tissues described by Nieuwkoop and Faber (1994). The expected rates of morphological changes in structures such as the gill, snout and tail were concurrently either delayed or accelerated by IOP exposure. These observations are consistent with what was observed in all five laboratories participating in the OECD Phase II validation of the AMA using IOP (OECD, 2007). These treatment-related effects on growth and development represent the AO in the AOP framework and form the basis for the overall linkage between putative DIO inhibition and adverse organismal effects.

Thyroid gland iodotyrosines/iodothyronines and nis gene expression

There was a significant increase in glandular MIT and DIT only in the 6.0 mg/L treatment at both 7 and 11 days (Figure 2A & 2B). T3 levels were significantly decreased in the 3.0 and 6.0 mg/L treatments only at 11 days (Figure 2C), whereas T4 levels were significantly increased in all treatments compared to control only at 11 days (Figure 2D). There was no effect on rT3 levels at either timepoint (Figure 2E). Normalized gene expression of *nis* mRNA showed a significant decrease compared to control in the 3.0 and 6.0 mg/L treatments at 7 days, with only the 3.0 mg/L treatment being significantly different than control at 11 days despite all treatments having lower, and more variable, expression levels than control (Figure 2F). Treatment-related increases in synthesis products (MIT, DIT, T4) provide evidence that the thyroid gland is not only capable of basal hormone synthesis during IOP exposure but is being stimulated to overproduce these products. This supports a plausible linkage between DIO inhibition and increased circulating TSH, despite the lack of a direct plasma TSH measurement.

Plasma thyroxine

Circulating T4 was significantly increased in the 3.0 and 6.0 mg/L treatments on both 7 and 11 days (Figure 3), although T4 levels were similarly increased in the 1.5 mg/L treatment but not statistically significant compared to control. Plasma T4 levels were elevated approximately 5-fold in all IOP treatments at 7 days of exposure and up to 10-fold at 11 days in the highest IOP treatment. Other potential circulating iodotyrosines/iodothyronines (MIT, DIT, T3, rT3, 3,5-T2, 3,3’-T2) were <LLOQ in all treatments and control. The marked increase in circulating T4 suggests that either T4 clearance is impaired, causing an accumulation of T4 in the plasma and/or affirmation of feedback within the hypothalamus-pituitary is impaired (i.e., TH resistance). This provides evidence of IOP-induced hyperthyroxinemia in the plasma compartment.

Iodothyronine deiodinase gene expression ontogeny

Pituitary, thyroid gland, liver, and hindlimb were collected from larvae in an independent spawn to characterize *dio* ontogeny. Gene expression profiles of *dio1*, *dio2.L*, *dio3.L* were examined at developmental stages spanning pre-metamorphosis (NF stage 51), thyroid-mediated pro-metamorphosis (≥NF stage 54), to just beyond metamorphic climax (NF stage 64). In the pituitary, *dio2.L* gene expression levels dominated throughout development at 15 to >30-fold higher than *dio1* and *dio3.L* (Figure 4A); *dio3.L* expression levels appear

to increase beyond NF stage 59 when plasma TH levels typically increase substantially to mediate metamorphosis. In the thyroid gland, all three *dio*s demonstrated similar expression levels up to NF stage 60 when *dio2.L* increased approximately 3-fold to NF stage 63 and then began to decrease at NF stage 64. At these later stages, NF stage 61 to 64, *dio3.L* increased steadily as *dio1* expression decreased to background levels (Figure 4B). In the liver, expression of *dio3.L* dominated in the early pro-metamorphic NF stages 54 to 58, then declined sharply to match basal expression levels of *dio1* and *dio2.L* by NF stage 60, remaining low through NF stage 66 (Figure 4C). In the hind limb, *dio2.L* expression dominated from NF stages 51 to 58 with a peak at NF stage 56 and slow downward trend to NF stage 58 (Figure 4D). Levels of *dio1* and *dio3.L* were minimal, hovering at baseline throughout this observation period (Figure 4D). If transcript abundance is an indicator of constitutive DIO activity in the various tissues throughout development, then these data support the enzyme-specific spatiotemporal vulnerability to inhibition by IOP and putative origins of systemic effects likely manifested via DIO inhibition.

DISCUSSION

Chemical hazard evaluation is transitioning away from routine animal testing and moving toward increased reliance on rapid alternative approaches such as high-throughput in vitro screening and in silico modeling (NRC, 2007; Thomas et al., 2019). However, in vitro chemical activity cannot be assumed to translate to adverse in vivo outcomes of regulatory concern without characterization of mechanistic linkages leading from a chemical-protein interaction to resulting biochemical perturbations and apical effects. Using *X. laevis* and a well-characterized model chemical, IOP, this study assembled the necessary data to support linkages between DIO inhibition in vitro, perturbed thyroid biochemistry in vivo, and impaired amphibian metamorphosis. These pathway-based linkages are critical to translating an in vitro response to an in vivo outcome important to ecological risk assessment.

IOP has been utilized to validate the in vivo AMA, a globally harmonized regulatory test guideline designed to identify chemicals with thyroid-mediated toxicity (OECD, 2009). However, use of IOP as a model chemical for assay validation poses several experimental challenges. In vivo, IOP has been shown to inhibit multiple DIO isoforms (Galton, 1989; Renko et al., 2012, 2015; Shintani et al., 2002), so the manifestation of in vivo effects could either be due to inhibition of one DIO predominantly causing the effects or a combination of multiple isoforms being inhibited by IOP concomitantly; developmental ontogeny of DIOs further complicates pathway-based interpretation of organismal effects. Structurally, IOP is iodinated and itself acts as a DIO substrate (Renko et al., 2012, 2015), so enzymatic liberation of iodine from IOP interferes with in vitro DIO screening assays utilized to understand relative potencies of chemicals toward these targets (Olker et al., 2019). As such, IOP could not be evaluated using the same assay methodology described in Olker et al. (2019). These challenges were directly addressed in the present study to leverage existing research with IOP as a model DIO inhibitor and to ascertain if chemical activity in vitro could be used to interpret mechanisms of adverse effects in vivo.

Over 1800 chemicals have been assessed in U.S.EPA's ToxCast program using in vitro screening assays for all three human DIO isoforms (Olker et al., 2019). A comparable *X.*

laevis DIO3 in vitro assay has also been implemented permitting calculations of relative potencies of a subset of ToxCast chemicals across orthologous assays (Mayasich et al., 2021). These assays rely upon enzymatic liberation of iodine from hormonal substrates – the Sandell-Kolthoff (SK) reaction is then used to generate a colorimetric readout proportional to the amount of iodine present (Renko et al., 2012, 2015). Iodine liberation from IOP confounds the interpretation of the SK readout in these assays. Therefore, to establish a relative potency of IOP toward DIOs comparable to other ToxCast chemicals, we instead quantified hormonal products generated by in vitro deiodinase activity using LC-MS/MS as an alternative readout. The results indicate that IOP inhibits hDIO1 and hDIO2 but neither ortholog of DIO3 in these assays (Figure 1), suggesting that in vivo effects caused by IOP exposure are less likely to be mediated through DIO3. The lack of IOP activity toward DIO3 in vitro is perplexing given that DIO3 has been shown to be inhibited by IOP in both *R. catesbeiana* (Galton, 1989) and *X. laevis* (Shintani et al., 2002) and IOP acts as a substrate of human DIO3 (Renko et al., 2015). If IOP indeed inhibits DIO3 in vivo, it is possible that the relative potency of IOP toward DIO3 is low enough that the in vitro screening assay conditions were not capable of identifying IOP as an inhibitor. The assay reaction conditions have been tailored to large-scale chemical screening amenable to high-throughput colorimetric readouts intended for characterizing relative potencies across chemical libraries, not necessarily for mimicking physiological conditions. Despite this inconsistency, the roles of DIO2 and DIO3 during amphibian metamorphosis have been well-established (Becker et al., 1997; Brown, 2005), while DIO1's role in metamorphosis remains unclear (Kuiper et al., 2006). The low potency of IOP toward DIO3 and lack of relevance of DIO1 implicates DIO2 as the predominant mediator of the in vivo effects observed in this study. Further, if DIO2 inhibition by IOP prevents T4-to-T3 conversion, then inhibition of this biochemical step precludes the importance of downstream DIO3-mediated inactivation of T3 to prevent its accumulation.

Larval exposure to IOP during metamorphosis caused increases in glandular MIT, DIT and T4 (Figure 2A, 2B, 2D, respectively), suggesting the thyroid gland is experiencing enhanced stimulation by TSH. However, decreases in glandular T3 (Figure 2C) suggests that DIO2 activity in the gland is impacted by IOP, which would normally account for a portion of T3 produced from T4. The remaining T3 is likely produced de novo from the hormone synthesis process, independent of DIO2 activity (Citterio et al., 2017). Gene expression levels (Figure 4B) indicate that all DIO isoforms are normally present in the thyroid gland and support the notion that IOP inhibition of DIO2 is likely occuring within the gland. The glandular rT3 levels (Figure 2E), together with the lack of in vitro inhibition of DIO3 suggests IOP is either not impacting constitutive thyroid DIO3 activity or, more likely, rT3 levels are a byproduct of the hormone synthesis process.

Interestingly, *nis* gene expression in the gland showed the opposite response from what would be expected under conditions of excess TSH stimulation (Figure 2F). Decreased abundance of *nis* transcripts has been shown previously in rats with acute and chronic iodide dosing as an escape mechanism from the Wolff-Chaikoff effect (Eng et al., 1999). In the current study, excess iodine present from deiodination of IOP appears to be modulating glandular *nis* expression in a conserved manner to regulate iodine uptake. This iodine-dependent alternative mechanism of gene regulation makes *nis* gene expression in this model

less useful as a consistent biomarker of TSH stimulation when the gland is subjected to excess iodine levels. Nonetheless, *nis* mRNA proves to be responsive to TSH stimulation and/or excess iodine levels and can be used as a diagnostic indicator of thyroid system perturbation when the proper context is understood.

Circulating T4 levels increased up to 10-fold higher compared to control by 11 days of exposure to IOP without any detection of circulating T3 (Figure 3). This directional response in circulating T4 is consistent with the directional responses reported in *R. catesbeiana* (Galton, 1989) and *X. laevis* (Huang et al., 2001) following exposure to IOP and suggests excess TSH stimulation of the gland is occurring. Despite an IOP-induced increase in circulating T4, previously reported expression of *tsh* mRNA in the pituitary continues unabated (Huang et al., 2001). Histopathology of thyroid glands following exposure to IOP as part of the phase II validation of the AMA showed mild to moderate increases in follicular cell hyperplasia and hypertrophy in the thyroid gland (OECD, 2007), consistent with an increase in TSH stimulation.

There is a body of literature indicating that the T4-to-T3 conversion by DIO2 is required to suppress TSH release from the pituitary as part of the regulatory feedback process (Huang et al., 2001; Larsen et al., 1979; Obregón et al., 1980). In the present study, pituitary *dio2.L* mRNA levels were orders of magnitude higher than the other isoforms throughout pre- and pro-metamorphosis (Figure 4A). The paradoxical rise in both circulating TH and TSH levels throughout normal pro-metamorphosis remains enigmatic and several hypotheses relating to the onset of regulatory feedback in the larval amphibian hypothalamic-pituitary-thyroid (HPT) axis have been proposed (Dodd and Dodd, 1976; Etkin, 1968; Huang et al., 2001; Sternberg et al., 2011). The question at hand here however is whether DIO2-mediated negative feedback is operable throughout pro-metamorphosis while circulating hormone levels are normally rising. If so, dramatic increases in circulating T4 and not T3, as observed in the present study, could be diagnostic of a DIO2-mediated thyrotoxic mechanism. The consistency of IOP-induced hyperthyroxinemia reported here and by others, together with the *dio2.L* ontogeny in the pituitary, and the failure of high T4 levels to suppress pituitary TSH release, all suggest that DIO2-mediated negative feedback is operable during pro-metamorphosis. However, the changing setpoint of negative feedback sensitivity to allow for concomitant increases of both TH and TSH levels during pro-metamorphosis must be controlled by other factors (e.g., pituitary DIO2/DIO3 expression levels [this study], growth hormone/prolactin [Shintani et al., 2002], corticotropin-releasing factor [Boorse and Denver, 2004; Denver, 1993], hypothalamic-pituitary maturation [Sternberg et al., 2011]). At metamorphic climax, the HPT axis switches to the classic mature negative feedback control by a mechanism that has yet to be fully elucidated (Huang et al., 2001; Shintani et al., 2002; Sternberg et al., 2011).

Although impaired feedback via DIO2 inhibition in the pituitary appears to cause the predominant biochemical effect signature measured here, T3 insufficiency, or hypothyroidism in the peripheral tissue compartment(s) is the more direct cause of abnormal growth and development. For example, metamorphosis of the gut, skin and tail are strongly correlated with upregulation of *dio2* expression (Becker et al., 1997, Cai and Brown, 2004, Galton and Hiebert, 1988, Galton, 1989) and can be induced to undergo precocious

metamorphosis by administration of T3 (Schreiber et al., 2005 [gut]; Wang and Brown, 1993 [tail]). Our study did not investigate intestinal development directly, but if DIO2 plays a critical role in gut development as suggested by these prior studies, then abnormal intestinal tract development could be contributing to the growth decrements observed with IOP exposure. Other adverse apical effects, presenting as asynchronous somatic development strongly suggest that metamorphosis of internal organs was also impaired. Further studies are necessary to confirm these possibilities.

Considering these data and observations across biological levels of organization as being dependent on a particular MIE can allow more informed prioritization of MIEs and categorization of in vitro chemical-activity signatures. In this study, developmental abnormalities were manifested through higher circulating T4 levels that imparted low-potency activation of TH receptors in specific tissues, together with localized DIO2 inhibition depriving tissues of high-potency T3 when critical to proper timing of metamorphosis. The lack of T3 present in tissues and blood precludes the significance of any potential DIO3 inhibition that may have been occurring despite IOP being dismissed as a low potency DIO3 inhibitor. Although DIO3 plays an important role in amphibian metamorphosis (Becker et al., 1997; Huang et al., 1999; Marsh-Armstrong et al., 1999; Shintani et al., 2002), this study suggests that potent inhibitors specific only to DIO3, and not additionally to DIO2, would need to be prioritized and interpreted in a category of their own. Whereas inhibitors of multiple DIOs, including potent DIO2 inhibition, would likely impart effects predominantly via DIO2 inactivity and need to be interpreted and categorized as such.

This study indicates that DIO2 inhibition during thyroid-mediated metamorphosis can lead to adverse effects including severe reductions in normal growth, developmental abnormalities, and delayed or arrested metamorphosis. Equipped with this information, we propose an AOP for DIO2 inhibition leading to altered amphibian metamorphosis (Figure 5; Haselman et al., 2021). Future work can leverage the biochemical data generated in this study, along with physicochemical properties of IOP as a potential reference chemical, to establish predictive relationships, aid the development of physiologically based computational models and provide a scientific basis for interpretation of in vitro DIO inhibition data.

Supplementary Material

Refer to Web version on PubMed Central for supplementary material.

Acknowledgements:

The authors would like to thank RaeAnn Schulte, Kelby Donnay and Carsten Knutsen for their technical contributions that were key to the success of the in vivo studies and data generation. Thanks to Philip DeGoey, Joseph O'Flanagan and Thomas Lerdall for their technical contributions key to the success of the in vitro screening assays. Recombinant *Xenopus laevis* DIO3 was kindly provided by Dr. Sally Mayasich. Additional thanks to Dr. Mary Gilbert and Mrs. Jenna Cavallin for thoughtful comments to improve this manuscript.

Data available at:

https://edg.epa.gov/metadata/catalog/main/home.page

REFERENCES

Becker KB, Stephens KC, Davey JC, Schneider MJ and Galton VA, 1997. The type 2 and type 3 iodothyronine deiodinases play important roles in coordinating development in Rana catesbeiana tadpoles. Endocrinology, 138(7), pp.2989–2997. [PubMed: 9202244]

Boorse GC and Denver RJ, 2004. Expression and hypophysiotropic actions of corticotropin-releasing factor in Xenopus laevis. General and comparative endocrinology, 137(3), pp.272–282. [PubMed: 15201065]

Braga M and Cooper DS, 2001. Oral cholecystographic agents and the thyroid. The Journal of Clinical Endocrinology & Metabolism, 86(5), pp.1853–1860. [PubMed: 11344170]

Brown DD, 2005. The role of deiodinases in amphibian metamorphosis. Thyroid, 15(8), pp.815–821. [PubMed: 16131324]

Cai L and Brown DD, 2004. Expression of type II iodothyronine deiodinase marks the time that a tissue responds to thyroid hormone-induced metamorphosis in *Xenopus laevis*. Developmental biology, 266(1), pp.87–95. [PubMed: 14729480]

Citterio CE, Veluswamy B, Morgan SJ, Galton VA, Banga JP, Atkins S, Morishita Y, Neumann S, Latif R, Gershengorn MC and Smith TJ, 2017. De novo triiodothyronine formation from thyrocytes activated by thyroid-stimulating hormone. Journal of Biological Chemistry, 292(37), pp.15434–15444. [PubMed: 28743746]

Denver RJ, 1993. Acceleration of anuran amphibian metamorphosis by corticotropin-releasing hormone-like peptides. General and comparative endocrinology, 91(1), pp.38–51. [PubMed: 8405889]

Dodd MHI and Dodd JM, 1976. The biology of metamorphosis. Physiology of the Amphibia, 3, pp.467–599.

Eng PH, Cardona GR, Fang SL, Previti M, Alex S, Carrasco N, Chin WW and Braverman LE, 1999. Escape from the acute Wolff-Chaikoff effect is associated with a decrease in thyroid sodium/iodide symporter messenger ribonucleic acid and protein. Endocrinology, 140(8), pp.3404–3410. [PubMed: 10433193]

Etkin W, 1968. Hormonal control of amphibian metamorphosis. Metamorphosis, a problem in developmental biology.

Fox J and Weisberg S (2019). An {R} Companion to Applied Regression, Third Edition. Thousand Oaks CA: Sage. URL: https://socialsciences.mcmaster.ca/jfox/Books/Companion/

Galton VA and Hiebert A, 1988. The ontogeny of iodothyronine 5'-monodeiodinase activity in *Rana catesbeiana* tadpoles. Endocrinology, 122(2), pp.640–645. [PubMed: 3257441]

Galton VA, 1989. The role of 3, 5, 3'-triiodothyronine in the physiological action of thyroxine in the premetamorphic tadpole. Endocrinology, 124(5), pp.2427–2433. [PubMed: 2785028]

Haselman J, Hornung M, Mayasich S Degitz S (2021). Type 2 iodothyronine deiodinase (Dio2) leading to altered amphibian metamorphosis. AOP-Wiki. Society for Advancement of AOPs. Available at: https://aopwiki.org/aops/190. Accessed August 12, 2021.

Haselman JT, Olker JH, Kosian PA, Korte JJ, Swintek JA, Denny JS, Nichols JW, Tietge JE, Hornung MW and Degitz SJ, 2020. Targeted pathway-based in vivo testing using thyroperoxidase inhibition to evaluate plasma thyroxine as a surrogate metric of metamorphic success in model amphibian Xenopus laevis. Toxicological Sciences, 175(2), pp.236–250. [PubMed: 32176285]

Hassan I, El-Masri H, Kosian PA, Ford J, Degitz SJ and Gilbert ME, 2017. Neurodevelopment and thyroid hormone synthesis inhibition in the rat: Quantitative understanding within the adverse outcome pathway framework. Toxicological Sciences, 160(1), pp.57–73. [PubMed: 28973696]

Hornung MW, Korte JJ, Olker JH, Denny JS, Knutsen C, Hartig PC, Cardon MC and Degitz SJ, 2018. Screening the ToxCast phase 1 chemical library for inhibition of deiodinase type 1 activity. Toxicological Sciences, 162(2), pp.570–581.\ [PubMed: 29228274]

Huang H, Marsh-Armstrong N and Brown DD, 1999. Metamorphosis is inhibited in transgenic Xenopus laevis tadpoles that overexpress type III deiodinase. Proceedings of the National Academy of Sciences, 96(3), pp.962–967.

Huang H, Cai L, Remo BF and Brown DD, 2001. Timing of metamorphosis and the onset of the negative feedback loop between the thyroid gland and the pituitary is controlled by type II iodothyronine deiodinase in Xenopus laevis. Proceedings of the National Academy of Sciences, 98(13), pp.7348–7353.

Kuiper GG, Klootwijk W, Morvan Dubois G, Destree O, Darras VM, Van der Geyten S, Demeneix B and Visser TJ, 2006. Characterization of recombinant Xenopus laevis type I iodothyronine deiodinase: substitution of a proline residue in the catalytic center by serine (Pro132Ser) restores sensitivity to 6-propyl-2-thiouracil. Endocrinology, 147(7), pp.3519–3529. [PubMed: 16601143]

Larsen PR, Dick TE, Markovitz BP, Kaplan MM and Gard TG, 1979. Inhibition of intrapituitary thyroxine to 3.5. 3'-triiodothyronine conversion prevents the acute suppression of thyrotropin release by thyroxine in hypothyroid rats. The Journal of clinical investigation, 64(1), pp.117–128. [PubMed: 447848]

Marsh-Armstrong N, Huang H, Remo BF, Liu TT and Brown DD, 1999. Asymmetric growth and development of the Xenopus laevis retina during metamorphosis is controlled by type III deiodinase. Neuron, 24(4), pp.871–878. [PubMed: 10624950]

Mayasich SA, Korte JJ, Denny JS, Hartig PC, Olker JH, DeGoey P, O'Flanagan J, Degitz SJ and Hornung MW, 2021. Xenopus laevis and human type 3 iodothyronine deiodinase enzyme cross-species sensitivity to inhibition by ToxCast chemicals. Toxicology in Vitro, 73, p.105141. [PubMed: 33713820]

Nieuwkoop PD, & Faber J (1994). Normal table of. Xenopus laevis, 252.

Noyes PD, Friedman KP, Browne P, Haselman JT, Gilbert ME, Hornung MW, Barone S Jr, Crofton KM, Laws SC, Stoker TE and Simmons SO, 2019. Evaluating chemicals for thyroid disruption: opportunities and challenges with in vitro testing and adverse outcome pathway approaches. Environmental health perspectives, 127(9), p.095001.

NRC, 2007. Toxicity testing in the 21st century: a vision and a strategy. National Academies Press.

Obregón MJ, Pascual A, Mallol J, ESCOBAR MD and REY FED, 1980. Evidence against a major role of L-thyroxine at the pituitary level: studies in rats treated with iopanoic acid (telepaque). Endocrinology, 106(6), pp.1827–1836. [PubMed: 7371594]

OECD (Organisation for Economic Cooperation and Development). 2007. Final Report of the Validation of the Amphibian Metamorphosis Assay - Phase 2: Multi-chemical Interlaboratory Study. In: OECD Environment, Health and Safety Publications Series on Testing and Assessment. No. 77.ENV/JM/MONO(2007)24. Paris, France: OECD. https://www.oecd.org/officialdocuments/publicdisplaydocumentpdf/?cote=ENV/JM/MONO(2007)24&docLanguage=En [Accessed 30 June 2021].

OECD. (2009). Test No. 231: Amphibian Metamorphosis Assay, OECD Guidelines for the Testing of Chemicals, Section 2, OECD Publishing, Paris, DOI: 10.1787/9789264076242-en.

OECD. (2015). Test No. 241: The Larval Amphibian Growth and Development Assay (LAGDA), OECD Guidelines for the Testing of Chemicals, Section 2, OECD Publishing, Paris. DOI: 10.1787/9789264242340-en.

Olker JH, Haselman JT, Kosian PA, Donnay KG, Korte JJ, Blanksma C, Hornung MW and Degitz SJ, 2018. Evaluating iodide recycling inhibition as a novel molecular initiating event for thyroid axis disruption in amphibians. Toxicological Sciences, 166(2), pp.318–331. [PubMed: 30137636]

Olker JH, Korte JJ, Denny JS, Hartig PC, Cardon MC, Knutsen CN, Kent PM, Christensen JP, Degitz SJ and Hornung MW, 2019. Screening the ToxCast phase 1, phase 2, and e1k chemical libraries for inhibitors of iodothyronine deiodinases. Toxicological Sciences, 168(2), pp.430–442. [PubMed: 30561685]

Paul Friedman K, Watt ED, Hornung MW, Hedge JM, Judson RS, Crofton KM, Houck KA and Simmons SO, 2016. Tiered high-throughput screening approach to identify thyroperoxidase inhibitors within the ToxCast phase I and II chemical libraries. Toxicological Sciences, 151(1), pp.160–180. [PubMed: 26884060]

Paul-Friedman K, Martin M, Crofton KM, Hsu CW, Sakamuru S, Zhao J, Xia M, Huang R, Stavreva DA, Soni V and Varticovski L, 2019. Limited chemical structural diversity found to modulate thyroid hormone receptor in the Tox21 chemical library. Environmental health perspectives, 127(9), p.097009.

R Core Team (2020). R: A language and environment for statistical computing. R Foundation for Statistical Computing, Vienna, Austria. URL https://www.R-project.org/.

Ritz C, Baty F, Streibig JC, Gerhard D (2015) Dose-Response Analysis Using R PLOS ONE, 10(12), e0146021 [PubMed: 26717316]

Renko K, Hoefig CS, Hiller F, Schomburg L and Köhrle J, 2012. Identification of iopanoic acid as substrate of type 1 deiodinase by a novel nonradioactive iodide-release assay. Endocrinology, 153(5), pp.2506–2513. [PubMed: 22434082]

Renko K, Schäche S, Hoefig CS, Welsink T, Schwiebert C, Braun D, Becker NP, Köhrle J and Schomburg L, 2015. An improved nonradioactive screening method identifies genistein and xanthohumol as potent inhibitors of iodothyronine deiodinases. Thyroid, 25(8), pp.962–968. [PubMed: 25962824]

Schreiber AM, Cai L and Brown DD, 2005. Remodeling of the intestine during metamorphosis of Xenopus laevis. Proceedings of the National Academy of Sciences, 102(10), pp.3720–3725.

Shintani N, Nohira T, Hikosaka A and Kawahara A, 2002. Tissue-specific regulation of type III iodothyronine 5-deiodinase gene expression mediates the effects of prolactin and growth hormone in Xenopus metamorphosis. Development, growth & differentiation, 44(4), pp.327–335.

Sternberg RM, Thoemke KR, Korte JJ, Moen SM, Olson JM, Korte L, Tietge JE and Degitz SJ Jr, 2011. Control of pituitary thyroid-stimulating hormone synthesis and secretion by thyroid hormones during Xenopus metamorphosis. General and comparative endocrinology, 173(3), pp.428–437. [PubMed: 21803044]

Swintek J, Flynn K, Haselman J, 2017. StatCharrms: Statistical Analysis of Chemistry, Histopathology, and Reproduction Endpoints Including Repeated Measures and Multi-Generation Studies. https://CRAN.R-project.org/package=StatCharrms

Therneau TM (2020). coxme: Mixed Effects Cox Models. R package version 2.2–16. https://CRAN.R-project.org/package=coxme

Thomas RS, Bahadori T, Buckley TJ, Cowden J, Deisenroth C, Dionisio KL, Frithsen JB, Grulke CM, Gwinn MR, Harrill JA and Higuchi M, 2019. The next generation blueprint of computational toxicology at the US Environmental Protection Agency. Toxicological Sciences, 169(2), pp.317–332. [PubMed: 30835285]

Tietge JE, Degitz SJ, Haselman JT, Butterworth BC, Korte JJ, Kosian PA, Lindberg-Livingston AJ, Burgess EM, Blackshear PE and Hornung MW, 2013. Inhibition of the thyroid hormone pathway in Xenopus laevis by 2-mercaptobenzothiazole. Aquatic toxicology, 126, pp.128–136. [PubMed: 23178179]

U.S. EPA. (2009). OCSPP 890.1100: Amphibian Metamorphosis Assay (AMA), Endocrine Disruptor Screening Program Test Guidelines, 890 series, www.regulations.gov, ID: EPA-HQ-OPPT-2009–0576.

U.S. EPA. (2015). OCSPP 890.2300: Larval Amphibian Growth and Development Assay (LAGDA), Endocrine Disruptor Screening Program Test Guidelines, 890 series, www.regulations.gov, ID: EPA-HQ-OPPT-2014–0766-0020.

Wang Z and Brown DD, 1993. Thyroid hormone-induced gene expression program for amphibian tail resorption. Journal of Biological Chemistry, 268(22), pp.16270–16278. [PubMed: 8344914]

Wang J, Hallinger DR, Murr AS, Buckalew AR, Simmons SO, Laws SC and Stoker TE, 2018. High-throughput screening and quantitative chemical ranking for sodium-iodide symporter inhibitors in ToxCast phase I chemical library. Environmental science & technology, 52(9), pp.5417–5426. [PubMed: 29611697]

Wang J, Hallinger DR, Murr AS, Buckalew AR, Lougee RR, Richard AM, Laws SC and Stoker TE, 2019. High-throughput screening and chemotype-enrichment analysis of ToxCast phase II chemicals evaluated for human sodium-iodide symporter (NIS) inhibition. Environment international, 126, pp.377–386. [PubMed: 30826616]

Wang J, Richard AM, Murr AS, Buckalew AR, Lougee RR, Shobair M, Hallinger DR, Laws SC and Stoker TE, 2021. Expanded high-throughput screening and chemotype-enrichment analysis of the phase II: e1k ToxCast library for human sodium-iodide symporter (NIS) inhibition. Archives of Toxicology, 95(5), pp.1723–1737. [PubMed: 33656581]

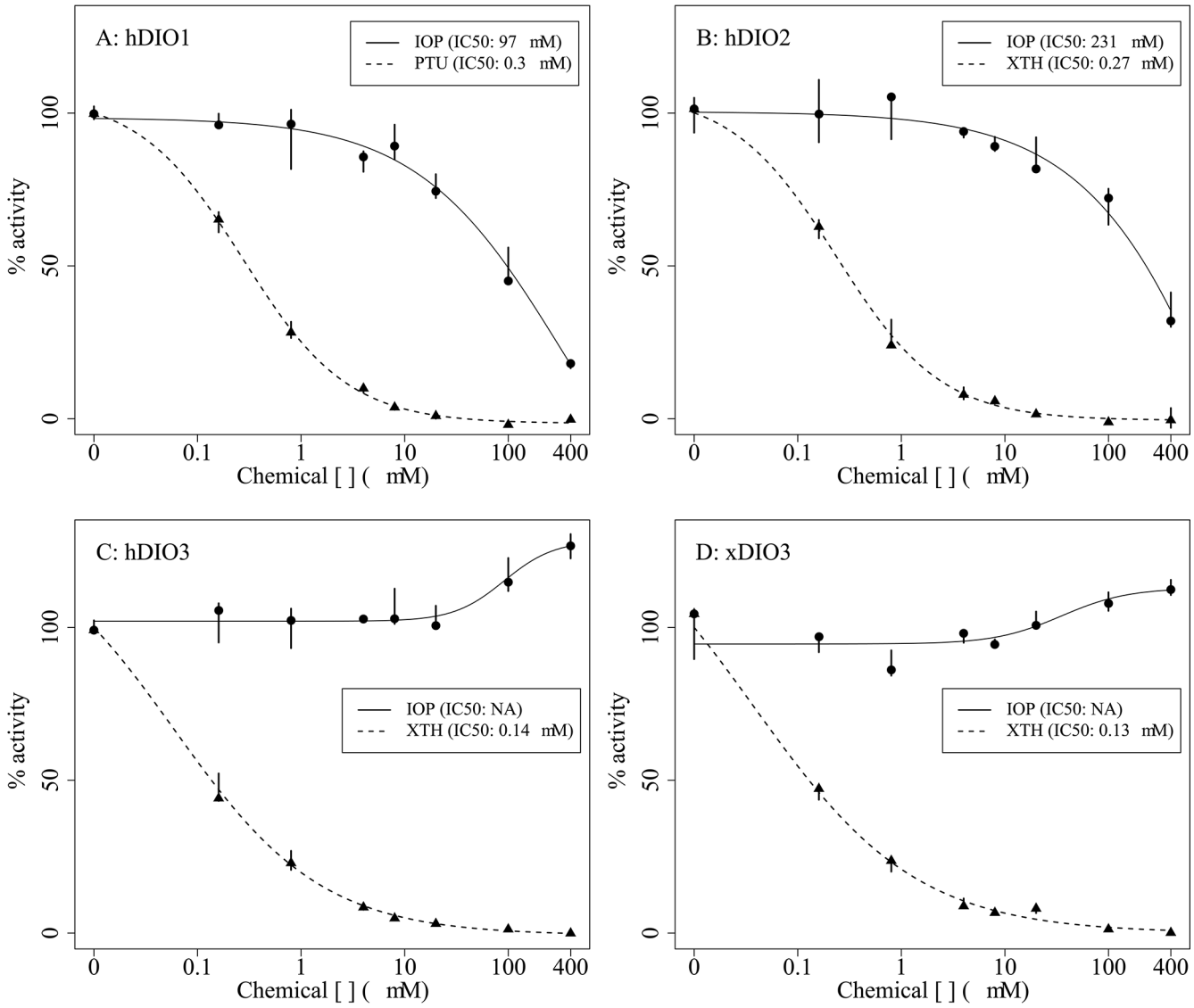

Figure 1.

Normalized in vitro concentration-responses and IC_{50}s for human type 1 deiodinase (hDIO1; A), human type 2 deiodinase (hDIO2; B), human type 3 deiodinase (hDIO3; C), *Xenopus laevis* type 3 deiodinase (xDIO3; D) enzyme activity when subjected to iopanoic acid (IOP) or model inhibitors, propylthiouracil (PTU) or xanthohumol (XTH). Points represent the median (n = 3), bars represent minimum and maximum values across the three replicate wells.

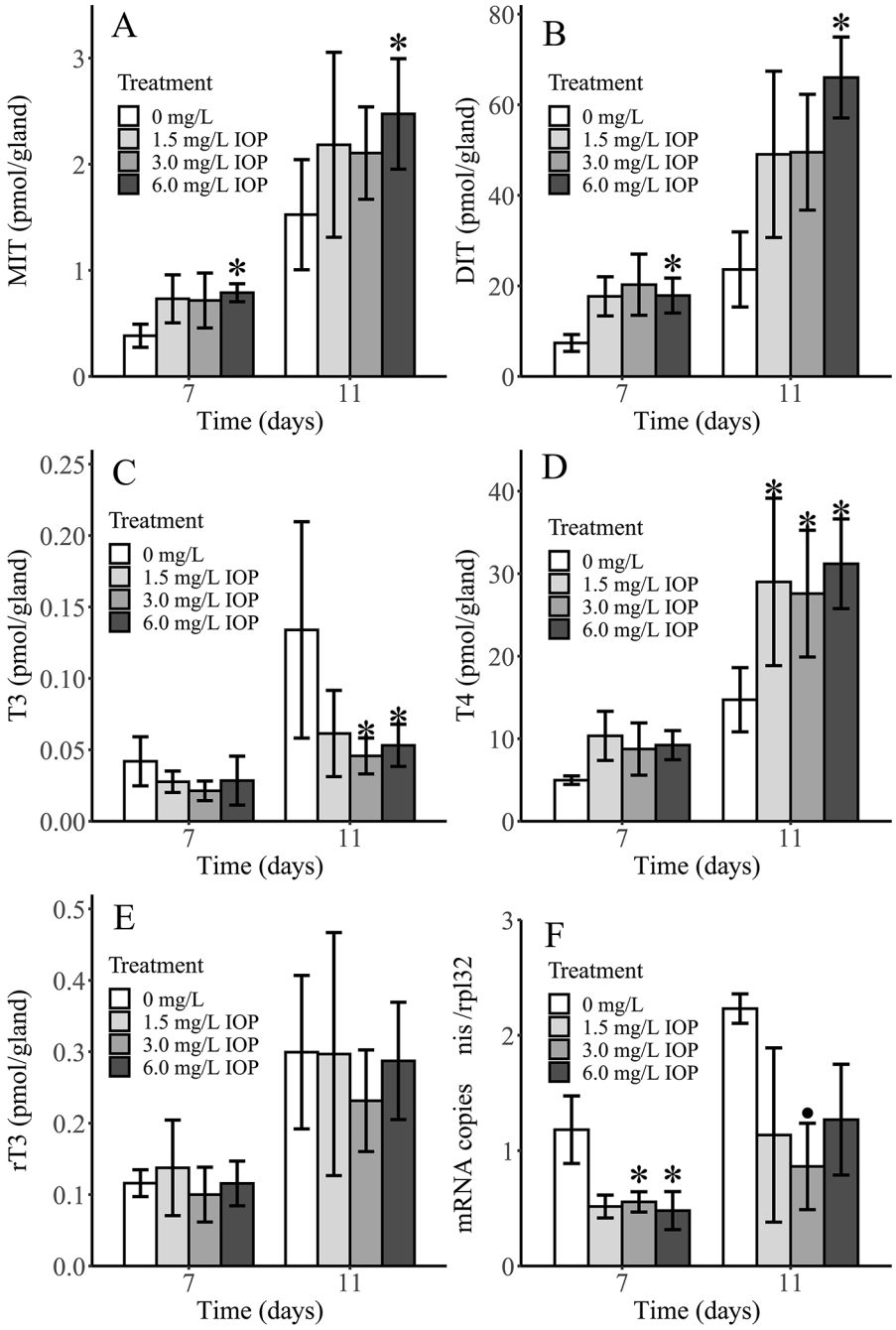

Figure 2.

Mean (n = 3 pools) thyroid gland levels of monoiodotyrosine (MIT; A), diiodotyrosine (DIT; B), triiodothyronine (T3; C), thyroxine (T4; D), reverse triiodothyronine (rT3; E) and normalized sodium-iodide symporter mRNA levels (*nis*; F) in thyroid glands of *Xenopus laevis* larvae after 7 and 11 days of exposure to iopanoic acid (IOP). Asterisk (*) indicates treatments that are significantly different than control based on Jonckheere-Terpstra ($p < 0.05$). Black circle (•) indicates treatment that is significantly different than control based on one-way ANOVA with Dunnett's test ($p < 0.05$). Error bars: SD.

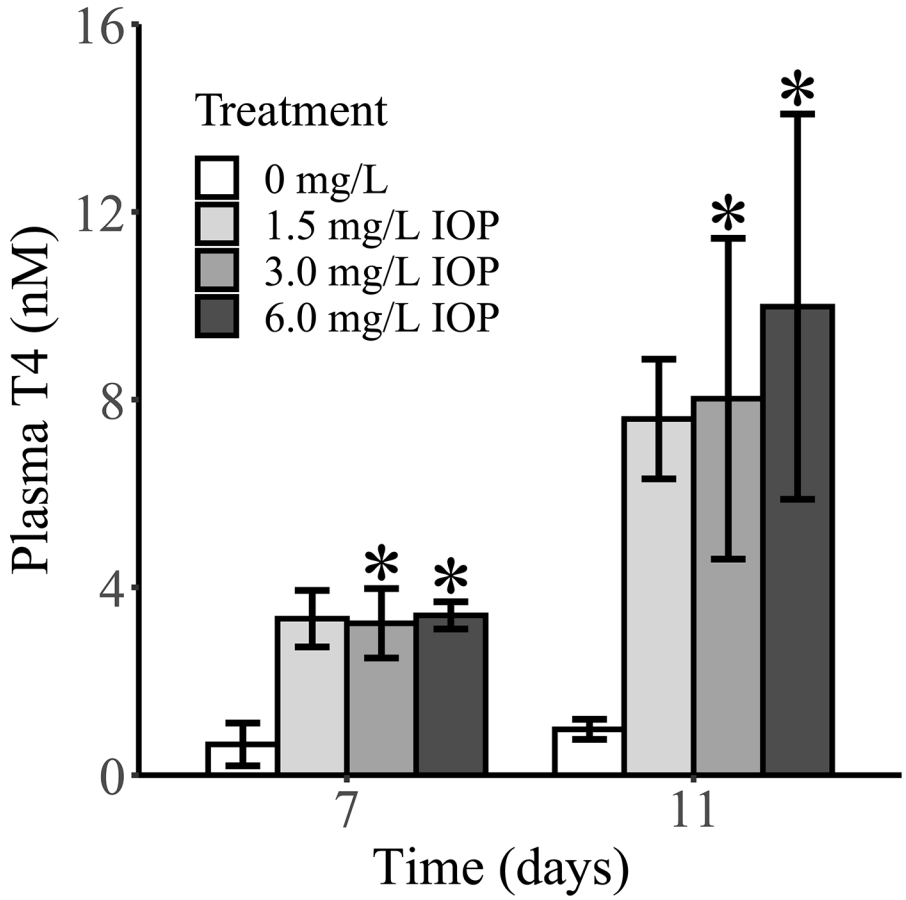

Figure 3.

Mean (n = 3 pools) plasma thyroxine (T4) levels in *Xenopus laevis* larvae following 7 and 11 days of exposure to iopanoic acid (IOP). Asterisks (*) indicate treatments that are significantly different than control based on Jonckheere-Terpstra trend test ($p < 0.05$). Error bars: SD. Other circulating iodotyrosines/iodothyronines (MIT, DIT, T3, rT3, 3,5-T2, 3,3'-T2) were <LLOQ in all treatments and control.

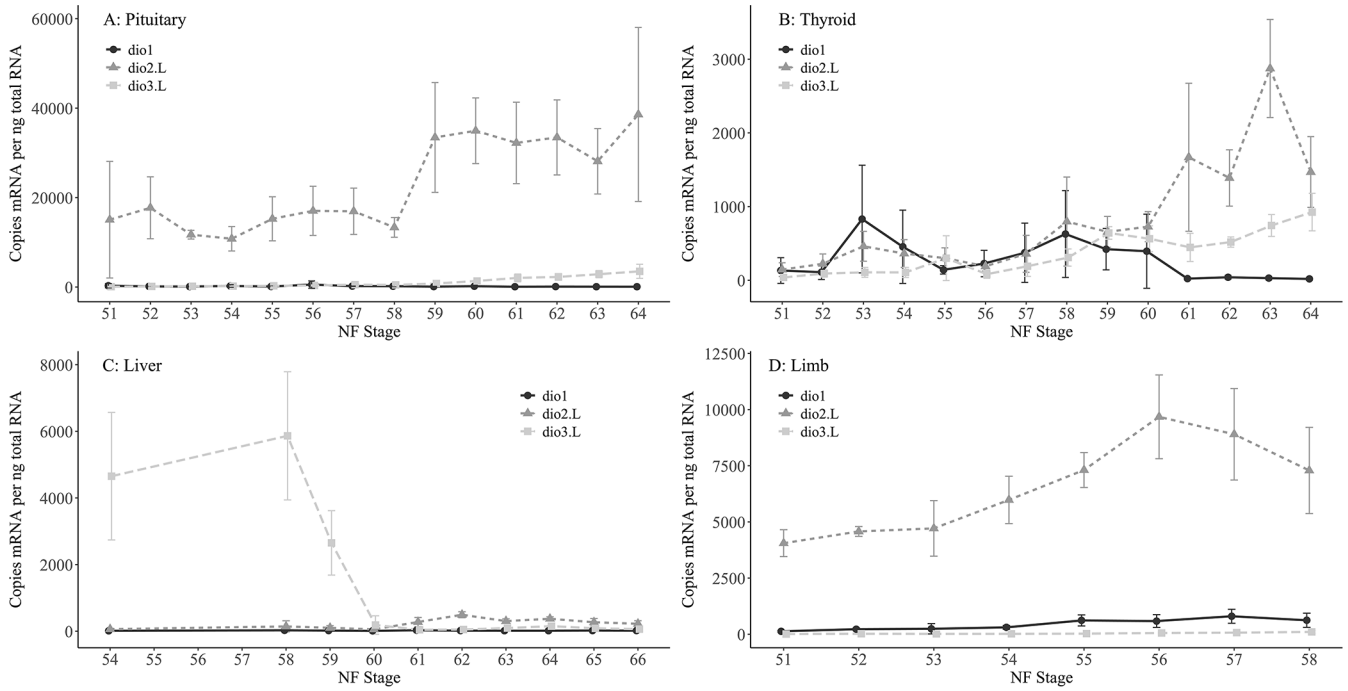

Figure 4.

Mean (n = 4 or 5 per stage) gene expression levels of types 1, 2 and 3 deiodinase (*dio1*, *dio2.L*, *dio3.L*) mRNA in *Xenopus laevis* pituitary (A), thyroid (B), liver (C), and limb (D) throughout metamorphic development. NF: Nieuwkoop and Faber (1994) developmental stage. Error bars: SD.

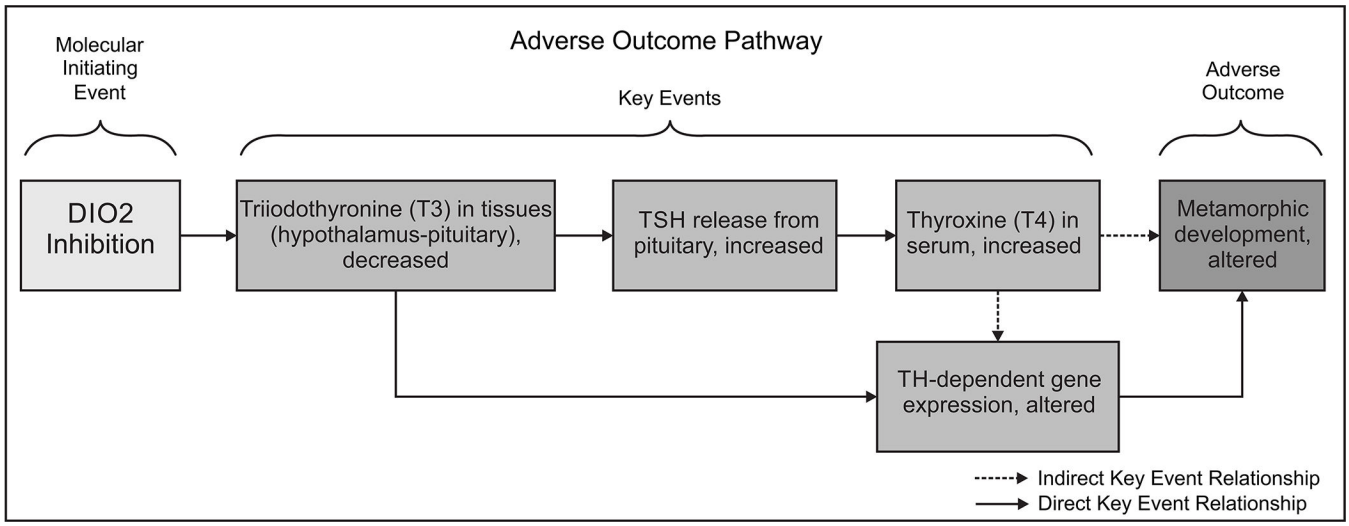

Figure 5.

Adverse Outcome Pathway 190: Type 2 iodothyronine deiodinase (DIO2) inhibition leading to altered amphibian metamorphosis. This is a simplified description of the mechanistic linkages starting from DIO2 inhibition, which mediates the thyroxine (T4: prohormone) to triiodothyronine (T3: active hormone) conversion. Inhibition of this biochemical step leads to both disruption of the hypothalamus-pituitary-thyroid negative feedback loop and disruption of T3-mediated processes in the peripheral tissues required for normal amphibian metamorphosis. Note that the key event, “TH-dependent gene expression, altered” is based on plausibility and scientific precedent, but is generally unrelated to the gene expression measured in this study.

Table 1.

Growth and developmental rates of pro-metamorphic *X. laevis* following exposure to iopanoic acid (IOP).

	Day 7		Day 11		Final sampling				
IOP treatment	**Mean mass (g) ± SD**	**N[a]**	**Mean mass (g) ± SD**	**N[a]**	**Mean mass (g) ± SD**	**Median days to NF66 (95% CI)**	**N[a] @ NF66**	**N[a] ≠ NF66**	**Mortalities**
Control	0.62 ± 0.08	24	0.90 ± 0.06	24	2.7 ± 0.09	27 (27, 28)	40	0	2
1.5 mg/L	0.62 ± 0.02	24	0.86 ± 0.07	24	2.0 ± 0.04	28 (27, 28)	39	0	3
3.0 mg/L	0.58 ± 0.04	24	0.78 ± 0.05 *	24	1.6 ± 0.18 *	28 (28, 29) †	41	0	1
6.0 mg/L	0.58 ± 0.02	24	0.82 ± 0.04 *	24	1.1 ± 0.07 *	32 (32, 33) †	20	21	1

[a] total number of larvae across three replicate tanks (days 7 and 11: n = 8 per tank; n = 14 per tank beyond day 11)

* significantly different than control based on Jonckheere-Terpstra trend test ($p < 0.05$)

† significantly different than control based on Cox mixed effects proportional hazard model ($p < 0.05$)

SD: standard deviation; NF: Nieuwkoop and Faber; CI: confidence interval